

This is a repository copy of *The ecology of wildlife disease surveillance: Demographic and prevalence fluctuations undermine surveillance*.

White Rose Research Online URL for this paper:

<https://eprints.whiterose.ac.uk/104540/>

Version: Accepted Version

Article:

Walton, Laura, Marion, Glenn, Davidson, Ross S. et al. (6 more authors) (2016) The ecology of wildlife disease surveillance: Demographic and prevalence fluctuations undermine surveillance. *Journal of Applied Ecology*. 1460–1469. ISSN 0021-8901

<https://doi.org/10.1111/1365-2664.12671>

Reuse

Other licence.

Takedown

If you consider content in White Rose Research Online to be in breach of UK law, please notify us by emailing eprints@whiterose.ac.uk including the URL of the record and the reason for the withdrawal request.

The Ecology of Wildlife Disease Surveillance: demographic and prevalence fluctuations undermine surveillance

| | |
|-------------------------------|--|
| Journal: | <i>Journal of Applied Ecology</i> |
| Manuscript ID | JAPPL-2015-00745.R1 |
| Manuscript Type: | Standard Paper |
| Date Submitted by the Author: | n/a |
| Complete List of Authors: | Walton, Laura; Biomathematics and Statistics Scotland, Marion, Glenn; Biomathematics and Statistics Scotland, Davidson, Ross; SRUC, White, Piran; University of York, Smith, Lesley; SRUC, Gavier-Widen, Dolores; Swedish University of Agricultural Sciences, Yon, Lisa; University of Nottingham, Hannant, Duncan; University of Nottingham, Hutchings, Michael; SRUC, |
| Key-words: | wildlife disease systems, wildlife ecology, disease surveillance, demographic fluctuations, wildlife populations, disease transmission models, stochastic population models |
| | |

**The Ecology of Wildlife Disease Surveillance: demographic and prevalence
fluctuations undermine surveillance**

**Laura Walton^{1,2,3}, Glenn Marion^{1*}, Ross S. Davidson², Piran C.L. White³, Lesley A. Smith², Dolores
Gavier-Widen⁴, Lisa Yon⁵, Duncan Hannant⁵ and Michael R. Hutchings²**

- 1. Biomathematics and Statistics Scotland, Edinburgh, United Kingdom
- 2. Disease Systems Team, SRUC, Edinburgh, United Kingdom
- 3. Environment Department, University of York, York, United Kingdom
- 4. Swedish University of Agricultural Sciences, Uppsala, Sweden
- 5. School of Veterinary Medicine and Science, University of Nottingham, United Kingdom

Email Addresses: Laura Walton: laura@bioass.ac.uk, Glenn Marion: glenn@bioass.ac.uk, Ross S. Davidson: ross.davidson@sruc.ac.uk, Piran C.L. White: piran.white@york.ac.uk, Lesley A. Smith: lesley.smith@sruc.ac.uk, Dolores Gavier-Widen: dolores.gavier-widen@slu.se, Lisa Yon: lisa.yon@nottingham.ac.uk, Duncan Hannant: duncan.hannant@nottingham.ac.uk, Michael R. Hutchings: mike.hutchings@sruc.ac.uk

***Correspondence author:** Glenn Marion, Biomathematics and Statistics Scotland, Peter Guthrie Tait Road, Edinburgh, EH9 3FD, UK. Telephone: +44 (0)131 650 4898. Fax: +44 (0)131 650 4901. E-mail: glenn@bioass.ac.uk

Running title: The Ecology of Wildlife Disease Surveillance

Word Count: 6979

26 Summary

27 1. Wildlife disease surveillance is the first line of defence against infectious disease. Fluctuations in
28 host populations and disease prevalence are a known feature of wildlife disease systems.
29 However, the impact of such heterogeneities on the performance of surveillance is currently
30 poorly understood.

31 2. We present the first systematic exploration of the effects of fluctuations prevalence and host
32 population size on the efficacy of wildlife disease surveillance systems. In this study efficacy is
33 measured in terms of ability to estimate long term prevalence and detect disease risk.

34 3. Our results suggest that for many wildlife disease systems fluctuations in population size and
35 disease lead to bias in surveillance-based estimates of prevalence and over-confidence in
36 assessments of both the precision of prevalence estimates and the power to detect disease.

37 4. Neglecting such ecological effects may lead to poorly designed surveillance and ultimately to
38 incorrect assessments of the risks posed by disease in wildlife. This will be most problematic in
39 systems where prevalence fluctuations are large and disease fade-outs occur. Such fluctuations
40 are determined by the interaction of demography and disease dynamics and although
41 particularly likely in highly fluctuating populations typical of fecund short lived hosts, can't be
42 ruled out in more stable populations of longer lived hosts.

43 5. *Synthesis and Applications:* Fluctuations in population size and disease prevalence should be
44 considered in the design and implementation of wildlife disease surveillance and the framework
45 presented here provides a template for conducting suitable power calculations. Ultimately
46 understanding the impact of fluctuations in demographic and epidemiological processes will
47 enable improvements to wildlife disease surveillance systems leading to better characterisation
48 of, and protection against endemic, emerging and re-emerging disease threats.

49 **Key-words:** wildlife disease systems, wildlife ecology, disease surveillance, demographic
50 fluctuations, wildlife populations, disease transmission models, stochastic population models

51 **Introduction**

52 Surveillance is the first line of defence against disease, whether to monitor endemic cycles of
53 infection (Ryser-Degiorgis 2013) or to detect incursions of emerging or re-emerging diseases (Kruse,
54 Kirkemo & Handeland 2004; Lipkin 2013)). Identification and quantification of disease presence and
55 prevalence is the starting point for developing disease control strategies as well as monitoring their
56 efficacy (OIE 2013). Knowledge of disease in wildlife is of considerable importance for managing risks
57 to humans (Daszak, Cunningham & Hyatt 2000; Jones *et al.* 2008) and livestock (Gortázar *et al.*
58 2007), as well as for the conservation of wildlife species themselves (Daszak, Cunningham & Hyatt
59 2000).

60
61 Recent public health concerns e.g. Highly Pathogenic Avian Influenza (Artois *et al.* 2009b) , Alveolar
62 Echinococcosis (Eckert & Deplazes 2004) and West Nile Virus (Brugman *et al.* 2013)), have led to a
63 growing recognition that current approaches need to be improved (Mörner *et al.* 2002). For
64 example, there is no agreed wildlife disease surveillance protocol shared among the countries in the
65 European Union (Kuiken *et al.* 2011). Furthermore several authors have identified the need for
66 improvements to the structure, understanding and evaluation of wildlife disease surveillance (Bengis
67 *et al.* 2004; Gortázar *et al.* 2007).

68
69 Much current practice for wildlife disease surveillance (Artois *et al.* 2009a) is based on ideas
70 developed for surveillance in livestock, including calculation of sample sizes needed for accurate
71 prevalence estimation (Grimes & Schulz 1996; Fosgate 2005) and detection of disease within a
72 population (Dohoo, Martin & Stryhn 2005). A common feature of these methods is that they assume
73 constant host populations and disease prevalence. These assumptions lead naturally to sample size
74 calculations (for both disease detection and prevalence estimation) which are based on a binomial
75 distribution and associated corrections for populations of finite size, such as the hyper-geometric
76 distribution (Artois *et al.* 2009a). (Fosgate 2009) reviewed current approaches to sample size

calculations in livestock systems and emphasised the importance of basing analyses on realistic assumptions about the system under surveillance.

Although constant population size and prevalence may often be reasonable assumptions for the analysis of livestock systems, they are considerably less tenable in wildlife disease systems, which are typically subject to much greater fluctuations in host population density and disease prevalence. Both sampling practicalities and changes in population density make it much harder to obtain a random sample of hosts of the desired sample size in wildlife disease surveillance programmes (Nusser *et al.* 2008), compared with livestock systems. It is not uncommon for wildlife disease surveillance to extend over several years and to test only a small fraction of the at risk population. For example, McGarry and co-workers report overall prevalence of zoonotic helminths in 42 brown rats (*Rattus norvegicus*) captured in a programme of active surveillance carried out in an urban area in England between 2008 and 2011 (McGarry *et al.* 2014). These authors also present comparable results from several studies in Europe and North America while another of the same host species conducted over a two year period across a broad area of Northwestern England captured just 133 individuals (Pounder *et al.* 2013). A notable example of passive surveillance i.e. the testing of found dead individuals, is that for zoonotic West Nile Virus (WNV) in wild birds across the whole of Great Britain during 2002-2009 in which only 2072 individuals representing 240 species were tested (Brugman *et al.* 2013).

The importance of temporal (Renshaw 1991; Wilson & Hassell 1997), spatial (Lloyd & May 1996; Tilman & Kareiva 1997) and other forms of heterogeneity (Read & Keeling 2003; Vicente *et al.* 2007; Davidson, Marion & Hutchings 2008) in population ecology has long been recognised (Anderson 1991; Smith *et al.* 2005), along with their role in the dynamics and persistence of infectious disease (Fenton *et al.* 2015). Detailed field observations have provided valuable insights into the temporal dynamics of wildlife disease systems. For example a study (Telfer *et al.* 2002) of cowpox virus in two

rodent host species at two sites over a four year period reveals strong temporal fluctuations in both population size and disease prevalence including disease fade-out (local extinction and re-emergence). Fade-outs are also observed in wildlife populations of longer lived mammals as shown by a six year study (Hawkins *et al.* 2006) of Devil Facial Tumour Disease in *Sarcophilus harrisii* (Tasmanian devil). One of the longest running and most intensive studies of disease in wildlife is the surveillance from 1982 to the present of TB in badgers at Woodchester Park, England where around 80% of the population is trapped tested and released annually (Delahay *et al.* 2000). These long term observations have revealed important insights into the dynamics of TB in badgers e.g. that infection within social groups is persistent whereas transmission between social groups is limited (Delahay *et al.* 2000). Parameter estimates derived from this study are used as a reference point for the simulation studies conducted below.

Despite these theoretical and empirical studies of temporal heterogeneities in wildlife disease systems, such effects have yet to be systematically accounted for, either in the design of surveillance programmes for wildlife disease systems, or in the analysis of the data obtained from them. Here we address this gap by using a non-spatial simulation model of a wildlife host population, subject to demographic fluctuations and pathogen transmission, in order to explore the impact of stochastic fluctuations in host demography and disease dynamics on the performance of surveillance. Two measures of surveillance performance are considered; estimation of long term prevalence and the ability (probability) to detect disease. Our results show that temporal fluctuations in wildlife disease systems limit the ability of surveillance to achieve both.

Methods

We develop a generic modelling framework that represents key features of surveillance in wildlife disease systems including essential aspects of demography, disease dynamics and surveillance design. This framework is described below along with three simulation studies that enable us to

explore the performance of surveillance across a wide range of scenarios representative of real world systems.

Stochastic Modelling framework

The model represents a host population subject to demographic fluctuations (births, deaths and immigration) and the transmission of a single pathogen. At each point in time t , the state-space represents the total population size $N(t)$, with $I(t)$ of these infected and $S(t) = N(t) - I(t)$ susceptible. The prevalence is then given by $p(t) = I(t)/N(t)$.

Demography. The birth rate of individuals is logistic, $rN(1 - N/k)$, with intrinsic growth rate r and carrying capacity k , reflecting the assumptions that population growth is resource limited. Individuals have a per capita death rate μ and immigration occurs at a constant rate ν .

Disease dynamics. A proportion γ of immigrants are infected, but otherwise all individuals enter the population (through birth or immigration) as susceptible, since we assume vertical and pseudo-vertical transmission are negligible. Susceptible individuals become infected at rate $\beta_0 S(t)$ through primary transmission (contact with infectious environmental sources including individuals outside the modelled population) and at rate $\beta S(t)I(t)$ by secondary transmission (contact with already infected individuals from within the population).

Disease surveillance. During a single period of surveillance (a *surveillance bout*), individuals are captured at per capita rate α , tested and released, and both the total number, and the number of infected individuals caught are recorded. Perfect diagnostic tests are assumed although limited sensitivities and specificities could be accounted for. A surveillance bout continues until a defined sample size m is obtained or some upper time limit has been reached. Such surveillance is most naturally considered in the context of active capture campaigns but could also be adapted to samples obtained from hunting and passive surveillance by accounting for the losses and sources of bias associated with such surveillance methods (see e.g. McElhinney *et al.* 2014).

Model implementation. The model framework is summarised in Table 1. Reported results are temporal averages (e.g. expected mean $E[M]$ and variance $\text{Var}[M]$ in population size) based on long run simulations following a burn-in period to allow the population to reach equilibrium where the effects of initial conditions are negligible. Within each run repeated surveillance bouts are simulated and the probability of detection PD is estimated as the proportion of bouts where disease is detected. The mean $E[\hat{p}_{surv}]$ and variance $\text{Var}[\hat{p}_{surv}]$ of the prevalence estimates averaged over repeated bouts are also recorded. We consider a continuous state-space implementation simulated by numerically integrating a set of stochastic differential equations (SDEs) and a discrete state-space implementation using the Gillespie algorithm (see Appendix S1 for details).

Simulation studies

Study 1 (results shown in Fig.1 and Fig.3) uses the SDE implementation and is designed to explore a generic but representative range of wildlife disease systems. Simulations were run for four values (0.01, 0.04, 0.1, 1.0) of the secondary transmission rate β . In each case the population death rate μ was varied over a wide range between 0.1 and 0.5, with the intrinsic growth rate set at $r=0.5$ so that, at the upper end of this range, populations are highly unstable. This gives rise to typical population sizes of 10-40 (see Fig.1a) and a wide range of disease prevalence. Similar results are obtained from simulations (not shown) where β is varied for a set of fixed values of μ where mortality rates span the interval $(0, r)$. Simulations not included here show that our results generalise, holding for transmission rates relative to a recovery rate (governing an additional transition from I to S) and death rates relative to birth rate, r . Different intensities of surveillance were simulated using four capture rates α (0.01, 0.1, 1.0, 10), for a sample size $m=10$. Full parameterisations for Fig.1 and Fig. 3 are shown in Tables S3 and S6 respectively.

Study 1a (results shown in Fig. 2) explores the effect of surveillance design using a subset of the parameter sets considered in study 1, namely $(\beta, \mu) = (1.0, 0.43); (1.0, 0.4);$ and $(0.1, 0.43)$. For each, a range of capture rates $\alpha = 0 \dots 10$ (with $m=10$) and a range of sample sizes $m=1, \dots$,

10000 (with $\alpha=0.1$) are considered. The values of all model parameters used are shown in Tables S4 and S5 (see Supporting Information).

Relevance to real wildlife disease systems. The intrinsic annual growth and death rates for badgers have been estimate as $r=0.6$ and $\mu=0.4$ (Anderson & Trewella 1985). Rescaling for $r=0.5$ as used in simulation study 1 corresponds to a rescaled $\mu=0.33$. In addition the secondary transmission rate for TB in badger populations was been estimated by the same authors to be $\beta=0.06-0.08$ assuming a density of badgers necessary for disease persistence is ~ 5 badgers km^{-2} (Anderson & Trewella 1985). The population size considered in simulation study 1 therefore corresponds to a surveillance area of around 8 km^2 . The range of parameters considered in study 1 places badgers towards the stable end of the spectrum. More fecund and shorter lived species would be expected to be less stable e.g. have higher mortality and secondary transmission rates. As noted earlier surveillance of badgers at Woodchester Park is relatively intensive leading to an annual probability of capture of around 80% corresponding to capture rates of $\alpha=1.6-2.2$ (Delahay *et al.* 2000). The population of *Sarcophilus harrisii* (Tasmanian devil) discussed earlier consisted of between 20-60 individuals and was subject to annual capture rates between 0.5 and 1.7 (Hawkins *et al.* 2006). Estimates of capture rates are not available for the larger scale studies referred to in the introduction (Brugman *et al.* 2013; Pounder *et al.* 2013; McGarry *et al.* 2014) but given the sample sizes obtained and the temporal and geographic scales involved it seems reasonable to assume that they are considerably lower. Simulation study 1 encompasses a wide range of real world wildlife disease surveillance.

Study 2 (results shown in Fig. 4) is designed to test the robustness of study 1 by exploring a wider range of scenarios: with intrinsic growth rates in the range (0,23); mortality rates in the range (0.25,14), carrying capacities in the range (0,36) and secondary contact rates in the range (0.01,5). Focussed on disease detection, results are conditioned on the presence of disease and simulations based on the Gillespie implementation which explicitly handles the discrete nature of small populations. The values of all model parameters used in Fig. 4 are shown in Table S7 (see Supporting Information).

Results

Estimating Prevalence

In order to develop an understanding of the properties of wildlife disease surveillance using the above model, we developed expressions describing prevalence estimates obtained by continuous surveillance, i.e. continuously deployed effort resulting in per capita capture rate α .

Consider the interval $[0, T]$ during which the population history is $\mathcal{H}[0, T] = \{(N(t), p(t)) : t \in [0, T]\}$, where $N(t)$ and $p(t)$ represent the population size and disease prevalence at time $t \in [0, T]$ respectively (see above). Let n_T represent the total number, and i_T the number of infected individuals sampled during this time interval. Conditional on the history $\mathcal{H}[0, T]$, the expectations of these quantities are:

$$E[n_T | \mathcal{H}[0, T]] = \int_0^T \alpha N(t) dt \quad \text{and} \quad E[i_T | \mathcal{H}[0, T]] = \int_0^T \alpha N(t) p(t) dt.$$

The surveillance estimate of disease prevalence is simply the ratio $\hat{p}_{surv}(T) = i_T / n_T$. Since immigration prevents extinction of the population and disease then the long time limit of this estimate can be equated with its expectation over all histories as follows:

$$\lim_{T \rightarrow \infty} \hat{p}_{surv}(T) = E[\hat{p}_{surv}] = \lim_{T \rightarrow \infty} \frac{\frac{1}{T} \int_0^T N(t) p(t) dt}{\frac{1}{T} \int_0^T N(t) dt} = \frac{E[N(t) p(t)]}{E[N(t)]}.$$

This can be re-expressed in the more suggestive form:

$$E[\hat{p}_{surv}] = E[p(t)] + \frac{Cov[N(t), p(t)]}{E[N(t)]} \quad (1)$$

Thus, when the covariance $Cov[N(t), p(t)] = E[N(t)p(t)] - E[N(t)]E[p(t)]$ between the population size and the prevalence is non-zero, the surveillance estimate of prevalence is a biased

estimate of the true prevalence, $E[p(t)]$. Since $Cov[N(t), p(t)]$ will be zero when either $N(t)$ or $p(t)$ are constant, we conclude that demographic fluctuations and stochasticity in disease dynamics undermine the efficacy of surveillance.

Effect of host demography and disease dynamics

Fig. 1 is based on simulation study 1 (see methods) and illustrates how population fluctuations and disease dynamics in the host-pathogen system affect the bias and variance of estimated prevalence. These results are generated by simulating the system, in each case until it reaches equilibrium, for a range of values of the death rate μ , with other parameters fixed. As the death rate increases, the equilibrium expected population size decreases and the relative size of the population fluctuations increase as measured by the coefficient of variation. For a given rate of disease transmission β , increasing the death rate reduces expected prevalence, and therefore simulating for different values of μ generates the range of prevalence values shown. The resulting relationship between demography and expected prevalence for particular disease characteristics (here a fixed transmission rate, β) is illustrated in Figs 1a & 1b. These figures show increasing population size and lower demographic fluctuations as expected prevalence increases (i.e. as μ decreases).

Fig. 1c shows the bias in the surveillance estimate of prevalence $E[\hat{p}_{surv}] - E[p(t)]$ obtained from the same set of simulations. Results shown are based on 10^6 surveillance bouts with sample size $m = 10$. The bias predicted by continuous sampling theory (which does not account for sample size) is also shown, and in this case accurately predicts simulated bias. Fig. 1c shows the bias in surveillance estimates of prevalence for four different transmission rates. For a given prevalence, populations associated with higher transmission rate (β) are more variable than those with lower transmission rate and therefore Fig. 1c shows that such variability increases the bias of surveillance estimates of disease prevalence. Fig. 1d shows the standard deviation in surveillance estimates of prevalence obtained from the same set of simulations. Comparison with the variability in prevalence estimates expected under the zero fluctuation assumption reveals that fluctuations in our simulated wildlife

disease system reduce the precision (increase the variance) of estimates obtained by surveillance. The variability of these estimates also increases with demographic fluctuations. Thus, in terms of prevalence estimation, the dynamics of the host-pathogen interaction are integral in determining the efficacy of surveillance. Assessment for a given system would require parameterisation of demography and disease dynamic, but the bias and variance in prevalence estimates shown in Fig. 1 are representative of a wide range of wildlife disease systems (see methods).

Additional studies shown in the supporting information confirm the qualitative impact of fluctuations in population and prevalence seen in Fig. 1 are robust to sample and population size and mode of secondary transmission. Fig. S1 shows analogous results with sample size 100, where environmental variability drives fluctuations in a population around 100 times larger than considered above. Fig. S3 shows results for simulation study 1 but where secondary transmission is frequency (as opposed to density) dependent. Fig. S5 and Fig. S6 show results from simulation study 1 with sample sizes 20 and 50 respectively.

Surveillance design

Based on simulation study 1a, Fig. 2 shows how the bias and variance of the estimate of prevalence changes as the intensity of surveillance (measured by the capture rate α) increases for fixed sample size (Figs 2a & 2c), and as the sample size, m , increases for a fixed capture rate (Figs 2b & 2d). For low capture rates, as $\alpha \rightarrow 0$ (and based on a fixed sample size), the continuous sampling estimate given in equation (1) provides an accurate prediction for the level of prevalence estimated from surveillance. As shown above, this is a biased estimate of the true prevalence $E[p(t)]$. However, increasing the capture rate reduces bias, and as α increases, this bias tends to zero. In addition, for large capture rates, the precision of the surveillance estimate of prevalence matches the variability of the underlying wildlife disease system (see Fig. 2c). Thus for low capture rates, the bias in surveillance estimates of prevalence is well described by continuous sampling theory (equation 1).

However, for larger capture rates, the properties of the surveillance estimate of prevalence increasingly reflect both the expected true prevalence (i.e. bias reduces), and the variability in the prevalence of the underlying disease system. In contrast, increasing sample size improves precision, but not bias (Fig. 2b). In comparison to the predictions from the standard binomial approach (which neglects fluctuations), these have lower precision, and improve less quickly with increasing sample size (see Fig. 2d). Additional simulation results (not shown) indicate that as the sample size increases, the capture rate required to obtain unbiased estimates increases. However, even for large sample sizes, when sampling is instantaneous sampling (i.e. $\alpha \rightarrow \infty$), the bias is zero and the standard deviation in the surveillance estimate of prevalence corresponds to that of the underlying wildlife disease system as shown above.

We previously noted that capture rates for relatively intensely monitored populations (Delahay *et al.* 2000; Hawkins *et al.* 2006) were between 0.5 and 2.2 with those of larger scale studies (Brugman *et al.* 2013; Pounder *et al.* 2013; McGarry *et al.* 2014) lower still. Therefore, the results of Fig. 2 suggest fluctuations will lead to bias in surveillance-based estimates of prevalence for a wide range of wildlife disease systems. However, the size of these effects will be dependent on the details of host species demography and disease dynamics.

The Probability of Detection

If prevalence is assumed constant and equal to the long term average prevalence $E[p]$ of the wildlife disease system, then the probability that disease is detected in a sample of size m is given by:

$$PD^{Bin} = f(E[p], m) = 1 - (1 - E[p])^m \quad (2)$$

This formula, based on simple binomial arguments, and variants that also assume constant prevalence, are the standard basis for sample size calculations (see e.g. Fosgate 2009). However, if prevalence fluctuates PD^{Bin} is a misleading estimate of the probability of detection.

When conducting surveillance prevalence will vary between the times when each of the m samples are collected, but we assume prevalence within a given surveillance bout is constant, and denoted p . Fig. 3a indicates that accounting only for fluctuations between surveillance bouts is an accurate approximation. Therefore, the expected probability of detection for sample size m is defined as

$$PD = E[f(p, m)] = E[1 - (1 - p)^m] \quad (3)$$

where the expectation is over the between bout prevalence distribution $P(p)$ which accounts only for prevalence fluctuations between surveillance bouts. For a single sample $m = 1$, equation (3) reduces to a linear form, so that $PD = PD^{Bin} = E[p]$. However, if $m > 1$, then equation (3) is non-linear, and therefore $PD \neq PD^{Bin}$. Further analysis of equation (3) e.g. suggesting $PD < PD^{Bin}$, is shown in Appendix S4 (see supporting information).

Effect of host demography and transmission dynamics

The results shown in Fig. 3 demonstrate the effect of host demography, transmission dynamics and surveillance design on the probability of detection. These results are obtained from the simulations described in Fig. 1, except for those in Fig. 3d where these simulations are rerun for different values of the capture rate (see study 1a in methods).

Fig. 3b illustrates an analytic calculation of PD based on approximating the between bout prevalence distribution $P(p)$ as a gamma distribution (see supporting information). Although, not completely successful, this does provide a more accurate prediction than PD^{Bin} . This approach could be used to

improve sample size calculations in situations where simulation is not possible, but information about prevalence fluctuations is available. Moreover, the results of Fig. 3a show that such approximations could be improved by assuming a more accurate representation of the prevalence distribution $P(p)$. Crucially, these calculations support the conclusion that the true probability of detection is less than that obtained when ignoring fluctuations i.e. less than PD^{Bin} . Fig. 3b also shows the impact of biased prevalence estimation on disease detection for the case $\beta = 0.1$. Fig. 1 demonstrates that in this case, surveillance results in inflated estimates of prevalence $E[\hat{p}_{surv}] > E[p(t)]$. Ignoring the effect of fluctuations would therefore lead to an estimated detection probability greater than PD^{Bin} , which is based on the true average prevalence $E[p]$.

Fig. 3c shows the effect of interactions between disease dynamics and demography. As in the case of prevalence estimation, conditioned on a given expected prevalence, larger contact rates β are associated with greater fluctuations in the underlying wildlife disease system (i.e. greater transmission rates are needed to sustain a given prevalence). Here larger fluctuations translate into reduced probability of detection. In Fig. 3c, for $\beta = 1.0$, the probability of detection is only a little above the line $PD = E[p]$; this corresponds to a single sample $m = 1$. Thus, in contrast to the zero fluctuation approximation PD^{Bin} , fluctuations reduce the effective sample size, for the $\beta = 1.0$ case from $m = 10$ to close to $m = 1$. Results not shown indicate that the reduction in effective sample size increases with sample size (and see Fig. 4). Fig. 3d shows the effect of capture rate on the probability of detection; counter intuitively, more intense surveillance effort actually reduces the probability of detection. This is consistent with the above observations regarding β ; less intense effort means that the required sample size takes longer to gather, which reduces between-bout fluctuations in prevalence.

Limits to disease detection in wildlife disease systems

The nature of host demography and disease dynamics in wildlife disease systems will often be poorly understood especially in cases of emerging disease. Fig. 4 is based on simulation study 2 (see methods) and shows the probability of detection associated with surveillance subject to demographic and disease fluctuations and the zero fluctuation approximation PD^{Bin} . This is done for two different sampling levels, and across a broader range of wildlife disease systems than considered above, each represented by one of the points on the graph. Depending on the level of fluctuations in the system, the effective sample size can range from the actual number of samples taken to $m \approx 1$. These results suggest that, when designing surveillance, ignoring the effect of fluctuations could lead to studies that are underpowered in their ability to detect disease. These results are consistent with those of Fig. 3 based on the SDE implementation.

Discussion

This paper represents the first systematic exploration of the impact of pathogen transmission dynamics and demographic aspects of host ecology on wildlife disease surveillance efficacy. We have introduced a framework within which surveillance design is characterised by the capture rate (α), in addition to the standard sample size (m). In this extended framework, the performance of surveillance is assessed in light of the ecology of the wildlife disease system of interest i.e. for particular population and disease parameters. The framework introduced here can thus serve as a template for performing power calculations that account for fluctuations in populations and disease prevalence for specific hosts and pathogens.

Our results show that surveillance design (choice of m and α) can have a large impact on bias and precision of prevalence estimation, and on the power to detect disease. With more unstable populations and greater fluctuations in disease, bias in prevalence estimates increases, and the precision of such estimates decreases. Such bias can be reduced by increasing capture rate, but for

fixed sample size this also reduces the ability to detect disease. However, results suggest that even in the most intensive wildlife disease surveillance programs (Delahay *et al.* 2000; Hawkins *et al.* 2006) typical capture rates are not sufficient to eliminate bias. In contrast, increasing sample size does not affect bias, but does improve statistical power in terms of both precision of prevalence estimates and disease detection. However, as sample size increases, such improvements in power are not as fast as would be expected if fluctuations were ignored, as they are in current surveillance design and analysis (Grimes & Schulz 1996; Dohoo, Martin & Stryhn 2005).

Surveillance is a critical prerequisite for defining and controlling wildlife disease risks, and our results suggest that ignoring significant temporal fluctuations in the design of wildlife disease surveillance generates inadequate assessments of risk. Moreover, the ecology of many wildlife species and the pathogens to which they are exposed lead to significant temporal fluctuations in both population size and disease prevalence (Anderson & May 1979; Anderson 1991; Renshaw 1991; Wilson & Hassell 1997; Telfer *et al.* 2002; Hawkins *et al.* 2006). The studies reported here were designed to explore these effects in a wide range of scenarios representative of actual surveillance in wildlife disease systems (see methods), and suggest that such issues are likely to be widespread. A key aspect not accounted for in the work presented here is disease induced mortality which preliminary results (not shown) suggest is likely to accentuate the effects shown here. Moreover, frequency dependent transmission and fluctuations driven by environmental variation, studied only briefly here, also reduced the efficacy of surveillance. The framework presented could also be extended to account for known extrinsic sources of bias, such as imperfect disease diagnostics, variation in habitat quality (Nusser *et al.* 2008; Walsh & Miller 2010) and biased capture rates (Tuytens *et al.* 1999) including aspects associated with passive surveillance.

There is much current interest in quantifying risks from wildlife disease (Daszak, Cunningham & Hyatt 2000; Jones *et al.* 2008), and this is stimulating debate on the need to improve wildlife disease

surveillance (Bengis *et al.* 2004; Butler 2006; Gortázar *et al.* 2007; Béneult, Ciliberti & Artois 2014). This paper will help to further inform this debate, highlighting the need to consider the ecology of wildlife disease systems when designing or analysing surveillance programs (Béneult, Ciliberti & Artois 2014). This assessment emphasizes the importance of accounting for temporal heterogeneities induced by population fluctuations and disease dynamics. Further research is needed to assess the impacts of ecology on wildlife disease surveillance including alternative and complimentary heterogeneities such as intrinsic and extrinsic forms of spatial heterogeneity, and other population structures. There is a wealth of literature describing the effects of such heterogeneity in ecology and epidemiology (Lloyd & May 1996; Tilman & Kareiva 1997; Keeling, Wilson & Pacala 2000; Read & Keeling 2003; Keeling 2005; Vicente *et al.* 2007), and our results suggest that these are likely to have important, but as yet unexplored, impacts on the efficacy of wildlife disease surveillance.

Acknowledgements

This work was supported by the European Commission under the Food, Agriculture and Fisheries, and Biotechnology Theme of the 7th Framework Programme for Research and Technological Development, grant agreement no. 222633. GM, RSD, LAS and MRH are grateful for funding from the Scottish Government's RESAS. We are grateful to the referees whose comments helped to significantly improve the manuscript.

Supporting Information

Additional Supporting Information may be found in the online version of this article :

Appendix S1: Model implementation

Appendix S2: Additional scenarios

Appendix S3: Analysis of disease detection probability

436

437 **Data Accessibility**

438 Model code is available at: DRYAD entry doi: tbc

439

For Peer Review

References

- Anderson, R. (1991) Populations and infectious diseases: ecology or epidemiology? *The Journal of Animal Ecology*, **60**, 1–50.
- Anderson, R. & May, R. (1979) Population biology of infectious diseases: Part I. *Nature*, **280**, 361–367.
- Anderson, R.M. & Trewheella, W. (1985) Population Dynamics of the Badger (*Meles meles*) and the Epidemiology of Bovine Tuberculosis (*Mycobacterium bovis*). *Philosophical Transactions of the Royal Society B: Biological Sciences*, **310**, 327–381.
- Artois, M., Bengis, R., Delahay, R.J., Duchêne, M.-J., Duff, J.P., Ferroglio, E., Gortazar, C., Hutchings, M.R., Kock, R.A., Leighton, F.A., Mörner, T. & Smith, G.C. (2009a) *Management of Disease in Wild Mammals* (eds RJ Delahay, GC Smith, and MR Hutchings). Springer Japan, Tokyo.
- Artois, M., Bicout, D., Doctrinal, D., Fouchier, R., Gavier-Widen, D., Globig, a, Hagemeijer, W., Mundkur, T., Munster, V. & Olsen, B. (2009b) Outbreaks of highly pathogenic avian influenza in Europe: the risks associated with wild birds. *Revue scientifique et technique (International Office of Epizootics)*, **28**, 69–92.
- Béneult, B., Ciliberti, A. & Artois, M. (2014) A Generic Action Plan against the Invasion of the EU by an Emerging Pathogen in Wildlife-A WildTech Perspective. *Planet@ Risk*, **2**, 174–181.
- Bengis, R.G., Leighton, F.A., Fischer, J.R., Artois, M. & Mörner, T. (2004) The role of wildlife in emerging and re-emerging zoonoses Recent emerging zoonoses Viral zoonoses. , **23**, 497–511.
- Brugman, V.A., Horton, D.L., Phipps, L.P., Johnson, N., Cook, A.J.C., Fooks, A.R. & Breed, A.C. (2013) Epidemiological perspectives on West Nile virus surveillance in wild birds in Great Britain. *Epidemiology and Infection*, **141**, 1134–1142.
- Butler, D. (2006) Disease surveillance needs a revolution. *Nature*, **440**, 6–7.
- Daszak, P., Cunningham, a a & Hyatt, a D. (2000) Emerging infectious diseases of wildlife--threats to biodiversity and human health. *Science (New York, N.Y.)*, **287**, 443–9.
- Davidson, R.S., Marion, G. & Hutchings, M.R. (2008) Effects of host social hierarchy on disease persistence. *Journal of theoretical biology*, **253**, 424–33.
- Delahay, R.J., Langton, S., Smith, G.C., Clifton-Hadley, R.S. & Cheeseman, C.L. (2000) The spatio-temporal distribution of *Mycobacterium bovis* (bovine tuberculosis) infection in a high-density badger population. *Journal of Animal Ecology*, **69**, 428–441.
- Dohoo, I., Martin, W. & Stryhn, H. (2005) Veterinary Epidemiologic Research. *Preventive Veterinary Medicine*, **68**, 289–292.
- Eckert, J. & Deplazes, P. (2004) Biological , Epidemiological , and Clinical Aspects of Echinococcosis , a Zoonosis of Increasing Concern. *clinical microbiology reviews*, **17**, 107–135.
- Fenton, A., Streicker, D.G., Petchey, O.L., Pedersen, A.B., Fenton, A., Streicker, D.G., Petchey, O.L. & Pedersen, A.B. (2015) Are All Hosts Created Equal ? Partitioning Host Species Contributions to Parasite Persistence in Multihost Communities. , **186**, 610–622.
- Fosgate, G.T. (2005) Modified exact sample size for a binomial proportion with special emphasis on diagnostic test parameter estimation. *Statistics in medicine*, **24**, 2857–66.
- Fosgate, G.T. (2009) Practical Sample Size Calculations for Surveillance and Diagnostic Investigations. *Journal of Veterinary Diagnostic Investigation*, **21**, 3–14.
- Gortázar, C., Ferroglio, E., Höfle, U., Frölich, K. & Vicente, J. (2007) Diseases shared between wildlife and livestock: a European perspective. *European Journal of Wildlife Research*, **53**, 241–256.
- Grimes, D.A. & Schulz, K.F. (1996) Determining sample size and power in clinical trials: the forgotten essential. *Seminars in reproductive endocrinology*, **14**, 125–31.
- Hawkins, C.E., Baars, C., Hesterman, H., Hocking, G.J., Jones, M.E., Lazenby, B., Mann, D., Mooney, N., Pemberton, D., Pyecroft, S., Restani, M. & Wiersma, J. (2006) Emerging disease and population decline of an island endemic, the Tasmanian devil *Sarcophilus harrisii*. *Biological Conservation*, **131**, 307–324.
- Jones, K.E., Patel, N.G., Levy, M. a, Storeygard, A., Balk, D., Gittleman, J.L. & Daszak, P. (2008) Global

- trends in emerging infectious diseases. *Nature*, **451**, 990–3.
- Keeling, M. (2005) The implications of network structure for epidemic dynamics. *Theoretical population biology*, **67**, 1–8.
- Keeling, M.J., Wilson, H.B. & Pacala, S.W. (2000) Space, Reinterpreting Lags, Functional Responses Models Ecological. , **290**, 1758–1761.
- Kruse, H., Kirkemo, A.-M. & Handeland, K. (2004) Wildlife as source of zoonotic infections. *Emerging infectious diseases*, **10**, 2067–72.
- Kuiken, T., Ryser-Degiorgis, M.P., Gavier-Widen, D. & Gortázar, C. (2011) Establishing a European network for wildlife. , **30**, 755–761.
- Lipkin, W.I. (2013) The changing face of pathogen discovery and surveillance. *Nature reviews. Microbiology*, **11**, 133–41.
- Lloyd, A.L. & May, R.M. (1996) Spatial Heterogeneity in Epidemic Models. *Journal of theoretical biology*, **179**, 1–11.
- McElhinney, L.M., Marston, D. a., Brookes, S.M. & Fooks, A.R. (2014) Effects of carcase decomposition on rabies virus infectivity and detection. *Journal of Virological Methods*, **207**, 110–113.
- McGarry, J.W., Higgins, A., White, N.G., Pounder, K.C. & Hetzel, U. (2014) Zoonotic Helminths of Urban Brown Rats (*Rattus norvegicus*) in the UK: Neglected Public Health Considerations? *Zoonoses and Public Health*, 44–52.
- Mörner, T., Obendorf, D.L., Artois, M. & Woodford, M.H. (2002) Surveillance and monitoring of wildlife diseases. *Revue scientifique et technique (International Office of Epizootics)*, **21**, 67–76.
- Nusser, S.M., Clark, W.R., Otis, D.L. & Huang, L. (2008) Sampling Considerations for Disease Surveillance in Wildlife Populations. *Journal of Wildlife Management*, **72**, 52–60.
- OIE. (2013) Terrestrial Animal Health Code
- Pounder, K.C., Begon, M., Sironen, T., Henttonen, H., Watts, P.C., Voutilainen, L., Vapalahti, O., Klempa, B., Fooks, A.R. & McElhinney, L.M. (2013) Novel hantavirus in field vole, United Kingdom. *Emerging infectious diseases*, **19**, 673–5.
- Read, J.M. & Keeling, M.J. (2003) Disease evolution on networks: the role of contact structure. *Proceedings. Biological sciences / The Royal Society*, **270**, 699–708.
- Renshaw, E. (1991) *Modelling Biological Populations in Space and Time*. Cambridge University Press.
- Ryser-Degiorgis, M.-P. (2013) Wildlife health investigations: needs, challenges and recommendations. *BMC veterinary research*, **9**, 223.
- Smith, K.F., Dobson, A.P., Mckenzie, F.E., Real, L.A., Smith, D.L. & Wilson, M.L. (2005) Ecological theory to enhance infectious disease control and public health policy.
- Telfer, S., Bennett, M., Bown, K., Cavanagh, R., Crespín, L., Hazel, S., Jones, T. & Begon, M. (2002) The effects of cowpox virus on survival in natural rodent populations: Increases and decreases. *Journal of Animal Ecology*, **71**, 558–568.
- Tilman, D. & Kareiva, P. (1997) *Spatial Ecology: The Role of Space in Population Dynamics and Interspecific Interactions*. Princeton University Press.
- Tuytens, F.A.M., Macdonald, D.W., Delahay, R., Rogers, L.M., Mallinson, P.J., Donnelly, C.A. & Newman, C. (1999) Differences in trappability of European badgers *Meles meles* in three populations in England. *Journal of Applied Ecology*, 1051–1062.
- Vicente, J., Delahay, R., Walker, N. & Cheeseman, C.L. (2007) Social organization and movement influence the incidence of bovine tuberculosis in an undisturbed high-density badger *Meles meles* population. *Journal of Animal ...*, **76**, 348–360.
- Walsh, D.P. & Miller, M.W. (2010) A weighted surveillance approach for detecting chronic wasting disease foci. *Journal of wildlife diseases*, **46**, 118–35.
- Wilson, H.B. & Hassell, M.P. (1997) Host – parasitoid spatial models : the interplay of demographic stochasticity and dynamics. *Proc. R. Soc. Lond. B*, **264**, 1189–1195.

Table 1: Model structure. Event, Rate and Effect on the State Space of the model. Conceptually the effect of each event affects an individual and this is reflected in the discrete nature of the corresponding changes in the state space. However, given this underlying conception of the model there are a number of different implementations which can be considered including via the Gillespie algorithm and stochastic differential equations (see text for details).

| Event | Rate | Effect |
|--|--------------------|--|
| Birth | $rN(1 - N/k)$ | $S \rightarrow S + 1$ |
| Death of Susceptible | μS | $S \rightarrow S - 1$ |
| Death of Infected | μI | $I \rightarrow I - 1$ |
| Susceptible Immigration | $(1 - \gamma) \nu$ | $S \rightarrow S + 1$ |
| Infected Immigration | $\gamma \nu$ | $I \rightarrow I + 1$ |
| Primary Transmission | $\beta_0 S$ | $S \rightarrow S - 1$ $I \rightarrow I + 1$ |
| Secondary Transmission | βIS | $S \rightarrow S - 1$ $I \rightarrow I + 1$ |
| Susceptible Active Capture and Release | αS | $S \rightarrow S$ |
| Infected Active Capture and Release | αI | $I \rightarrow I$ |

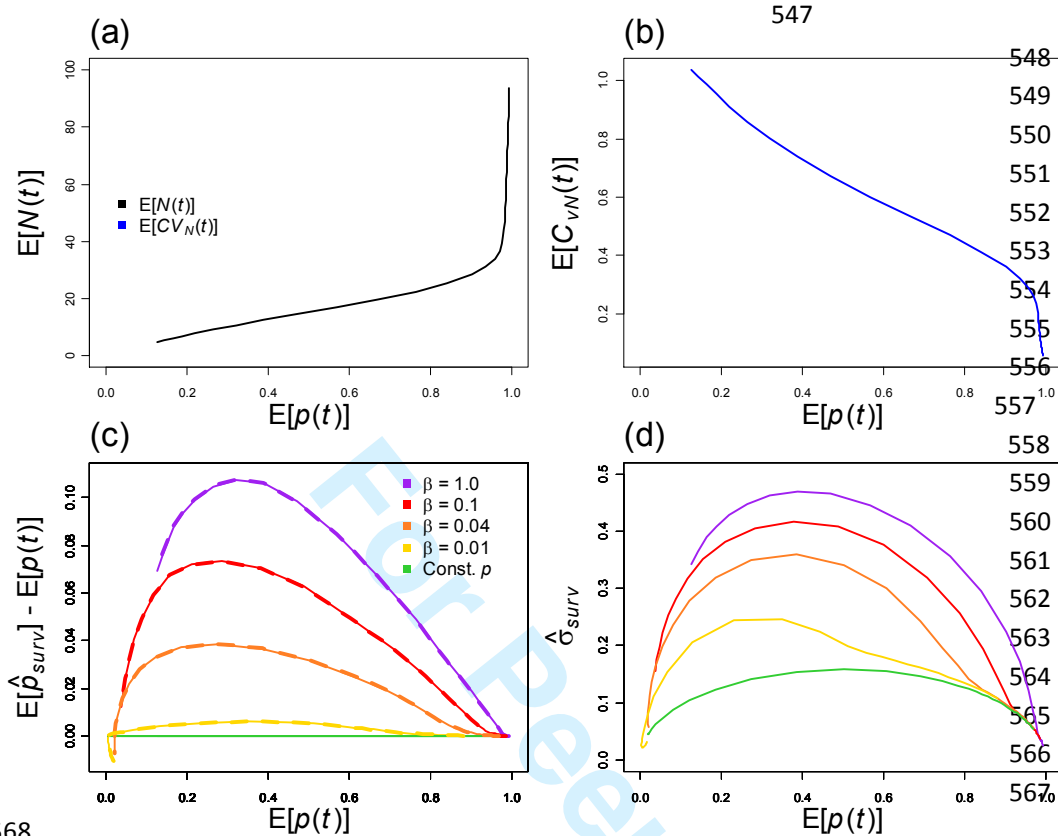


Figure 1: Effect of host demography and disease transmission. Data are shown for a range of values of the death rate μ which controls the stability and size of the population, and thus determines disease prevalence for a given transmission rate, β . For $\beta=1$ plot 1.a shows that expected population size increases with expected prevalence $E[p(t)]$ (i.e. as μ decreases) whilst plot 1.b shows that the coefficient of variation of the population size decreases. For the four values of β indicated and fixed sample size $m=10$, plot 1.c shows the bias $E[\hat{p}_{surv}] - E[p(t)]$, and plot 1.d the standard deviation in surveillance estimates of prevalence, versus the expected value of true disease prevalence in the system, $E[p(t)]$. Results shown are based on 10^6 surveillance bouts using the SDE implementation of the model (see text) using the set of parameter values described in Appendix S2.

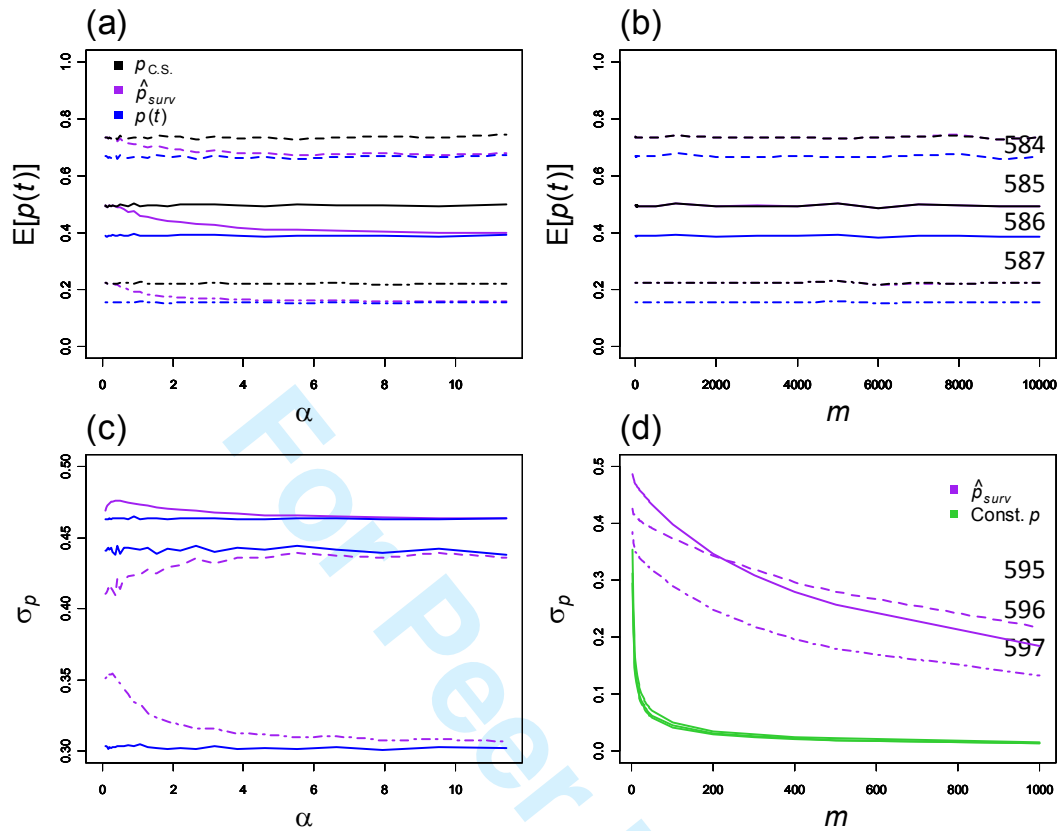


Figure 2: Effect of surveillance design. In all plots results are shown for three wildlife disease systems with (β, μ) : (1, 0.43) solid lines; (1, 0.4) dashed; and (0.1, 0.43) dot-dashed. Plots (a) and (b) show expected values of the surveillance estimate of prevalence (purple), the true prevalence (blue) and the continuous sampling theory prediction (black, see text for details). Plots (c) and (d) show the expected standard deviation (denoted, σ_p) in both the true (blue) and the surveillance estimated (purple) prevalence. (a) and (c) are plotted against a range of values of the capture rate α , for $m = 10$, and (b) and (d) versus a range of sample sizes m for $\alpha = 0.1$. Plot (d) also shows the constant prevalence estimate of the standard deviation based on the binomial (green). Parameter values used are as described in Table S3 (see Supporting Information).

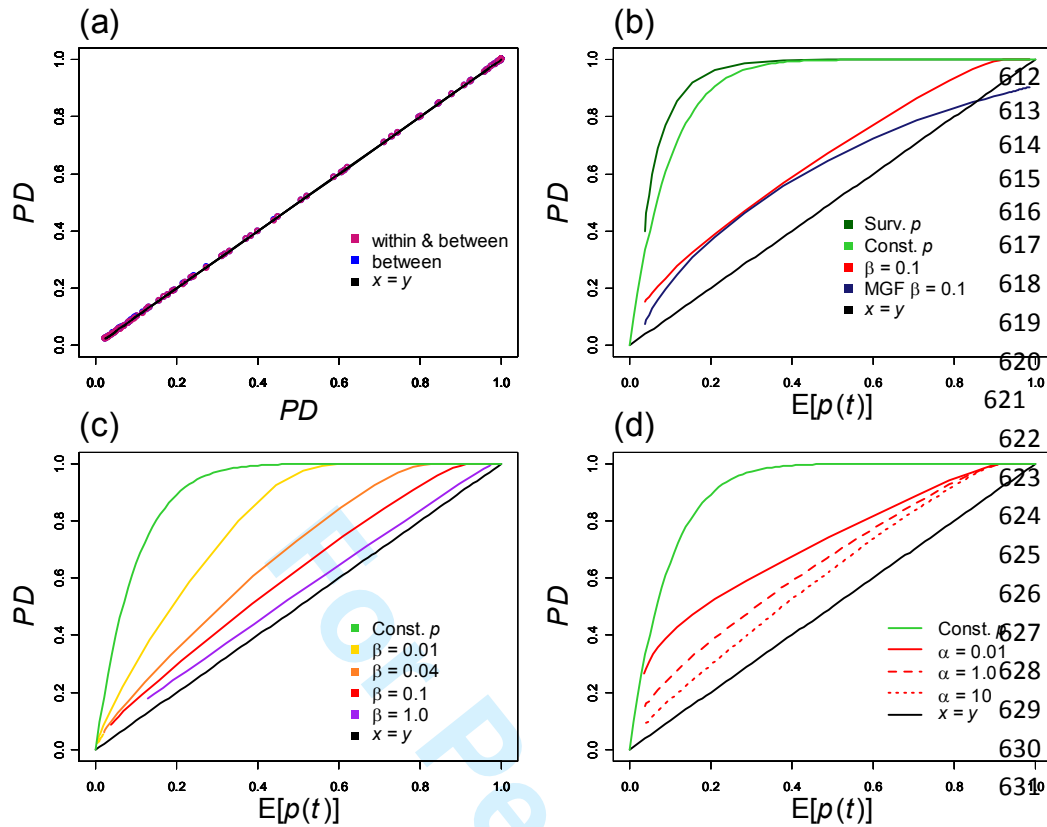


Figure 3: Effect of host-pathogen and surveillance dynamics on probability of detection. Results based on simulations used for Figure 1 (for details see Table S4, Appendix S2). (d) estimated PD versus approximations based on modifications of equation (3) accounting for fluctuations in prevalence (i) within and between bouts and (ii) between bouts only. (c) shows PD^{Bin} based on both $E[p]$ (green) and $E[\hat{p}_{surv}]$ (black) and (for $\beta = 0.1$) PD and the approximation (equation 4) based on an assumed gamma distribution. (a) shows PD^{Bin} (green) and PD for various values of β (as shown yellow ($\beta = 0.01$); orange ($\beta = 0.04$); red ($\beta = 0.1$); purple ($\beta = 1.0$)) versus actual prevalence $E[p]$. (b) shows PD^{Bin} (green) and PD for $\beta = 0.1$ and the three capture rates $\alpha = 0.01, 1.0, 10$. In (a), (b) and (c) the black line indicates $PD = E[p(t)]$.

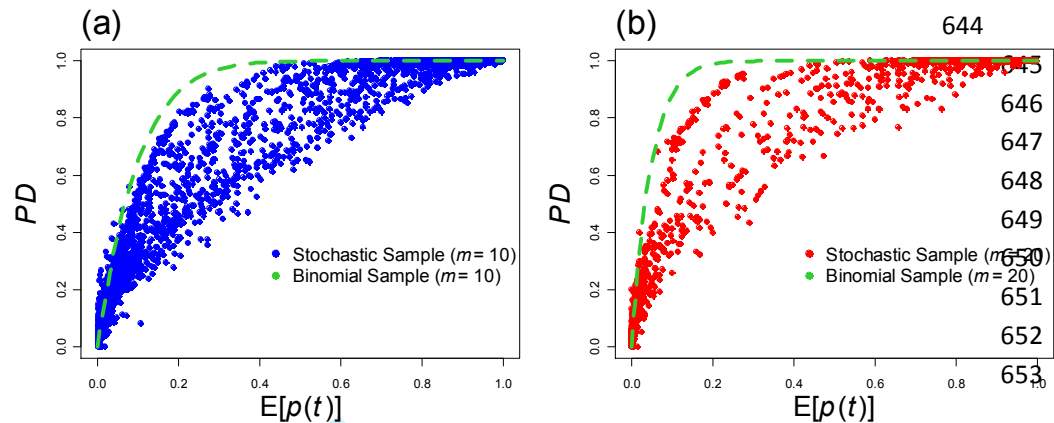


Figure 4: Fluctuations reduce power to detect disease: The two panels show the probability that disease is detected (conditional on non-zero prevalence) for target sample sizes 10 and 20. Each coloured dot represents the average of 100-1000 realisations of the model implemented using the Gillespie algorithm that met the sample target for a particular combination of parameters representing a distinct host-pathogen system (for details see Table S5, Appendix S2). The green dashed line in both graphs represents PD^{Bin} the probability of detection assuming constant prevalence (see equation 2). It can be seen that PD^{Bin} generally over-estimates the power of the sample in that it predicts a larger probability of detection than is realised in the stochastic simulations.

Supporting Information:**The Ecology of Wildlife Disease Surveillance:****Demographic and prevalence fluctuations undermine surveillance**

Laura Walton^{1,2,3}, Glenn Marion^{1*}, Ross S. Davidson², Piran C.L. White³, Lesley A. Smith², Dolores Gavier-Widen⁴, Lisa Yon⁵, Duncan Hannant⁵ and Michael R. Hutchings²

1. Biomathematics and Statistics Scotland, Edinburgh, United Kingdom
2. Disease Systems Team, SRUC, Edinburgh, United Kingdom
3. Environment Department, University of York, York, United Kingdom
4. Swedish University of Agricultural Sciences, Uppsala, Sweden
5. School of Veterinary Medicine and Science, University of Nottingham, United Kingdom

Appendix S1. Model implementation**Model implementation**

The model is implemented as a set of coupled Stochastic Differential Equations, (SDEs) (see e.g. Mao 1997) and simulated using the Euler-Maruyama algorithm (e.g. see Higham 2001) which is essentially a generalisation of the Euler discretisation for Ordinary Differential Equations to SDEs. The model is also implemented (for simulation study 2) as a continuous-time discrete-state space Markov process, simulated using Gillespie's algorithm (Gillespie 1976). The Gillespie algorithm is an event-based method that makes use of the fact that in the underlying discrete state-space Markov process at any point in time the waiting time between events is exponential and parameterised by the total rate of all possible events i.e. the sum of all possible events. The Gillespie algorithm proceed from time t by drawing a waiting time τ from this distribution, advancing time to $t + \tau$, and then selects the nature of the event at random but weighted according to the relative rates of the possible events. The SDE implementation has been constructed so that it is the diffusion limit of the Gillespie implementation, ensuring that the results are consistent between the two implementations (see below). The Gillespie algorithm is computationally more intensive; by contrast, using SDEs is faster and therefore

facilitates both more accurate estimation of model statistics (i.e. a greater number of surveillance bouts can be run) and more extensive exploration of parameter space. However, the discrete nature of the state-space under the Gillespie algorithm is a more direct implementation of the model described in Table 1, and provides a more accurate representation of population dynamics especially for small populations.

Relationship between discrete and continuous (SDE) state-space model implementations.

In this appendix we describe the relationship between the continuous time discrete state-space Markov process and the stochastic differential equation (SDE) implementations of the model described in the main text.

Our starting point is the SI model described in Table 1 (main text) implemented as a continuous time discrete state-space Markov process in which the number of infected individuals $I(t)$ and total population size $N(t) = S(t) + I(t)$, are represented as integer variables. The Gillespie algorithm exploits the fact that the time between events is distributed exponentially with parameter $R(t)$ given by the sum of all the event rates in Table 1 and the probability that a given event occurs is given by the associated event rate divided by $R(t)$.

However, under this implementation one can also consider the expectation and variance-covariance of the change in the state-space variables $I(t)$ and $N(t)$ during a small time interval. For convenience denote the state of the system at time t by $X(t) = \{I(t), N(t)\}$. Then for example, conditional on the state of the system at time t , the expected change in the population size associated with birth events from time t to $t + \delta t$ is given by $E_B[\delta N(t) | X(t)] = rN(t) (1 - N(t)/k) \delta t$. Similarly, the variance in δN associated with birth events is $\text{Var}_B[\delta N(t)] = rN(t) (1 - N(t)/k) \delta t + O(\delta t^2)$, and henceforth we will assume δt is sufficiently small to ignore the higher order terms. In the model described in the main text (see Table 1 and surrounding text) all individuals are born susceptible and therefore birth does not affect the infective population size $I(t)$ i.e. $E_B[\delta I(t) | X(t)] = 0$, $\text{Var}_B[\delta I(t)] = 0$, and $\text{Cov}_B[\delta I(t), \delta N(t) | X(t)] = 0$. However, migration of infectives affects both $I(t)$ and $N(t)$ and to first order in δt we find that $E_{mI}[\delta N(t) | X(t)] = \gamma \nu \delta t$, $\text{Var}_{mI}[\delta N(t)] = \gamma \nu \delta t$, $E_{mI}[\delta I(t) | X(t)] = \gamma \nu \delta t$, $\text{Var}_{mI}[\delta I(t)] = \gamma \nu \delta t$ and $\text{Cov}_{mI}[\delta I(t), \delta N(t) | X(t)] = \gamma \nu \delta t$. The full set of first- and second-order statistics describing changes in the state-space associated with each event type are given (up to first order in δt) in Table S1.

| Etype | Event | $E[\delta N X(t)]$ | $E[\delta I X(t)]$ | $\text{Var}[\delta N X(t)]$ | $\text{Var}[I X(t)]$ | $\text{Cov}[\delta N, \delta I X(t)]$ |
|-------|-------------------------|-------------------------|---------------------|-----------------------------|----------------------|---------------------------------------|
| B | Birth | $rN(1 - N/k)\delta t$ | 0 | $rN(1 - N/k)\delta t$ | 0 | 0 |
| DS | Death of Susceptible | $-\mu S\delta t$ | 0 | $\mu S\delta t$ | 0 | 0 |
| DI | Death of Infected | $-\mu I\delta t$ | $-\mu I\delta t$ | $\mu I\delta t$ | $\mu I\delta t$ | $\mu I\delta t$ |
| mS | Susceptible Immigration | $(1 - \gamma)v\delta t$ | 0 | $(1 - \gamma)v\delta t$ | 0 | 0 |
| ml | Infected Immigration | $\gamma v\delta t$ | $\gamma v\delta t$ | $\gamma v\delta t$ | $\gamma v\delta t$ | $\gamma v\delta t$ |
| 1ry | Primary Transmission | 0 | $\beta_0 S\delta t$ | 0 | $\beta_0 S\delta t$ | 0 |
| 2ry | Secondary Transmission | 0 | $\beta I S\delta t$ | 0 | $\beta_0 S\delta t$ | 0 |

Table S1: Expectations and variance-covariances in changes (during the time interval t to $t+\delta t$) to the state space $\{I(t), N(t)\}$ associated with each event type in the discrete state-space model described in the main text (see Table 1). All such quantities are shown to first order in δt . Note: capture and release events are omitted since they affect neither $I(t)$ or $N(t)$.

We now show how to construct a continuous time, continuous state-space (diffusion) version of the model which is consistent with above implementation in that it preserves the means and variance-covariance statistics shown in Table S1. To do so we construct a set of stochastic differential equations (SDEs) which we later solve numerically in discrete time steps (e.g. see Higham 2001). The following Itô stochastic differential equations represent the change in the system state variables during an infinitesimally small time interval dt

$$\begin{aligned}
 dN(t) = & \left(f_{N,B}(X(t)) + f_{N,DS}(X(t)) + f_{N,DI}(X(t)) + f_{N,mS}(X(t)) + f_{N,ml}(X(t)) \right. \\
 & + f_{N,1ry}(X(t)) + f_{N,2ry}(X(t)) \Big) dt \\
 & + g_{N,B}(X(t))dB_B(t) + g_{N,DS}(X(t))dB_{DS}(t) + g_{N,DI}(X(t))dB_{DI}(t) \\
 & + g_{N,mS}(X(t))dB_{mS}(t) + g_{N,ml}(X(t))dB_{ml}(t) \\
 & + g_{N,1ry}(X(t))dB_{1ry}(t) + g_{N,2ry}(X(t))dB_{2ry}(t) \\
 \\
 dI(t) = & \left(f_{I,B}(X(t)) + f_{I,DS}(X(t)) + f_{I,DI}(X(t)) + f_{I,mS}(X(t)) + f_{I,ml}(X(t)) \right. \\
 & + f_{I,1ry}(X(t)) + f_{I,2ry}(X(t)) \Big) dt
 \end{aligned}$$

$$\begin{aligned}
& + g_{I,B}(X(t))dB_B(t) + g_{I,DS}(X(t))dB_{DS}(t) + g_{I,DI}(X(t))dB_{DI}(t) \\
& + g_{I,mS}(X(t))dB_{mS}(t) + g_{I,mI}(X(t))dB_{mI}(t) \\
& + g_{I,1ry}(X(t))dB_{1ry}(t) + g_{I,2ry}(X(t))dB_{2ry}(t)
\end{aligned}$$

Here the quantities $B_B(t)$, $B_{DS}(t)$, $B_{DI}(t)$, $B_{mS}(t)$, $B_{mI}(t)$, $B_{1ry}(t)$, $B_{2ry}(t)$ are independent Brownian motions corresponding to each of the seven event types and the correct interpretation of these equations requires consideration of associated stochastic integrals (Mao, 1997). For small but finite dt the quantities $dB_B(t)$, $dB_{DS}(t)$, $dB_{DI}(t)$, $dB_{mS}(t)$, $dB_{mI}(t)$, $dB_{1ry}(t)$, $dB_{2ry}(t)$ can be interpreted as independent draws from a zero mean Gaussian with variance dt for each event type and each time point $0, dt, 2dt, \dots, T \in (0, T)$. Thus e.g. $E[dB_B(t)] = 0$, $E[dB_B(t)dB_B(t)] = 0$ and $E[dB_B(t)dB_{DS}(t)] = 0$. This discretisation is the basis for the numerical simulation of these SDEs used in this paper.

The so-called drift, $f_{N,B}(X(t))$, $f_{N,DS}(X(t))$, $f_{N,DI}(X(t))$, $f_{N,mS}(X(t))$, $f_{N,mI}(X(t))$, $f_{N,1ry}(X(t))$, $f_{N,2ry}(X(t))$ and diffusion, $g_{N,B}(X(t))$, $g_{N,DS}(X(t))$, $g_{N,DI}(X(t))$, $g_{N,mS}(X(t))$, $g_{N,mI}(X(t))$, $g_{N,1ry}(X(t))$, $g_{N,2ry}(X(t))$, terms representing changes in the variable $N(t)$ and the corresponding quantities representing changes in $I(t)$ are deterministic functions of the state-space $X(t)$ determined as follows.

Given the nature of the Brownian motions taking the expectation of the above equations yields

$$\begin{aligned}
E[dN(t)|X(t)] & = \left(f_{N,B}(X(t)) + f_{N,DS}(X(t)) + f_{N,DI}(X(t)) + f_{N,mS}(X(t)) + f_{N,mI}(X(t)) \right. \\
& \quad \left. + f_{N,1ry}(X(t)) + f_{N,2ry}(X(t)) \right) dt \\
E[dI(t)|X(t)] & = \left(f_{I,B}(X(t)) + f_{I,DS}(X(t)) + f_{I,DI}(X(t)) + f_{I,mS}(X(t)) + f_{I,mI}(X(t)) \right. \\
& \quad \left. + f_{I,1ry}(X(t)) + f_{I,2ry}(X(t)) \right) dt
\end{aligned}$$

Which suggests that for each event type $Etype$ $f_{N,Etype}(X(t))$ and $f_{I,Etype}(X(t))$ should be interpreted as the mean update shown in Table S1 for $N(t)$ and $I(t)$ respectively. For example, $f_{N,1ry}(X(t))$ and

$f_{N,2ry}(X(t))$ are both zero since only birth, death and migration change the population size, i.e. neither primary nor secondary infection changes the population size.

The variance in the update for $N(t)$ is given by

$$\text{Var}[dN(t)|X(t)] = E[dN(t)^2|X(t)] - E[dN(t)|X(t)]^2$$

However, we have just shown that $E[dN(t)|X(t)]$ is of order dt and therefore to first order in dt we can write

$$\begin{aligned} \text{Var}[dN(t)|X(t)] &= E[dN(t)^2|X(t)] = \\ &g_{N,B}(X(t))^2 dt + g_{N,DS}(X(t))^2 dt + g_{N,DI}(X(t))^2 dt + g_{N,mS}(X(t))^2 dt \\ &+ g_{N,mI}(X(t))^2 dt + g_{N,1ry}(X(t))^2 dt + g_{N,2ry}(X(t))^2 dt \end{aligned}$$

and

$$\begin{aligned} \text{Var}[dI(t)|X(t)] &= E[dI(t)^2|X(t)] = \\ &g_{I,B}(X(t))^2 dt + g_{I,DS}(X(t))^2 dt + g_{I,DI}(X(t))^2 dt + g_{I,mS}(X(t))^2 dt \\ &+ g_{I,mI}(X(t))^2 dt + g_{I,1ry}(X(t))^2 dt + g_{I,2ry}(X(t))^2 dt \end{aligned}$$

Here we have made use of the independent nature of the Brownian motions described above.

These last two equations therefore suggest that for each event type E_{type} , $g_{N,E_{type}}(X(t))^2$ and $g_{I,E_{type}}(X(t))^2$ should be interpreted as the variance in update shown in Table S1 for $N(t)$ and $I(t)$ respectively.

The above calculations are summarised in Table S2. Comparison with Table S1 allows the functional form for each drift and diffusion term to be identified.

Finally, the covariance

$$\text{Cov}[dN(t)dI(t)|X(t)] = E[dN(t)dI(t)|X(t)] - E[dN(t)|X(t)]E[dI(t)|X(t)]$$

to first order in dt is given by

$$\begin{aligned} \text{Cov}[dN(t)dI(t)|X(t)] &= E[dN(t)dI(t)|X(t)] = \\ &+ g_{N,DI}(X(t))g_{I,DI}(X(t))dt + g_{N,mI}(X(t))g_{I,mI}(X(t))dt \end{aligned}$$

where we have shown only the non-zero terms. Comparison with the functional forms for the diffusion terms described above shows that this expression is consistent with the covariance terms shown in Table S1.

| Etype | $E[dN X(t)]$ | $E[dI X(t)]$ | $\text{Var}[dN X(t)]$ | $\text{Var}[dI X(t)]$ | $\text{Cov}[dN,dI X(t)]$ |
|-------|---------------------|---------------------|-----------------------|-----------------------|----------------------------------|
| B | $f_{N,B}(X(t))dt$ | $f_{I,B}(X(t))dt$ | $g_{N,B}(X(t))^2dt$ | $g_{I,B}(X(t))^2dt$ | 0 |
| DS | $f_{N,DS}(X(t))dt$ | $f_{I,DS}(X(t))dt$ | $g_{N,DS}(X(t))^2dt$ | $g_{I,DS}(X(t))^2dt$ | 0 |
| DI | $f_{N,DI}(X(t))dt$ | $f_{N,DI}(X(t))dt$ | $g_{N,DI}(X(t))^2dt$ | $g_{I,DI}(X(t))^2dt$ | $g_{N,DI}(X(t))g_{I,DI}(X(t))dt$ |
| mS | $f_{N,mS}(X(t))dt$ | $f_{I,mS}(X(t))dt$ | $g_{N,mS}(X(t))^2dt$ | $g_{I,mS}(X(t))^2dt$ | 0 |
| mI | $f_{N,mI}(X(t))dt$ | $f_{I,mI}(X(t))dt$ | $g_{N,mI}(X(t))^2dt$ | $g_{I,mI}(X(t))^2dt$ | $g_{N,mI}(X(t))g_{I,mI}(X(t))dt$ |
| 1ry | $f_{N,1ry}(X(t))dt$ | $f_{I,1ry}(X(t))dt$ | $g_{N,1ry}(X(t))^2dt$ | $g_{I,1ry}(X(t))^2dt$ | 0 |
| 2ry | $f_{N,2ry}(X(t))dt$ | $f_{I,2ry}(X(t))dt$ | $g_{N,2ry}(X(t))^2dt$ | $g_{I,2ry}(X(t))^2dt$ | 0 |

Table S2: Expectation and variance-covariances in changes (during the time interval t to $t+dt$) to the state space $\{I(t),N(t)\}$ associated with each event type in the SDE model as described in Appendix S1. All such quantities are shown to first order in dt . Comparison with Table S1 enables both drift e.g. $f_{N,B}(X(t))$ and diffusion e.g. $g_{N,B}(X(t))$ functions to be identified. Note: capture and release events are omitted since they affect neither $I(t)$ or $N(t)$.

References

Higham, D. J. (2001) An Algorithmic Introduction to Numerical Simulation of Stochastic Differential Equations. *SIAM REVIEW* **43**(3), 525–546

Mao, X., (1997) *Stochastic Differential Equations and Applications*. Horwood, New York.

For Peer Review

Appendix S2. Parameterisations used.

This section of the appendix describes in detail the parameter combinations used to produce the graphs in the main text. Values of the form: a,b,c,d etc refer to discrete values used for different lines shown on the Figures. Values of the form a;b;c refer to smallest value; largest value; step size describing the range of values (e.g. of the death rate) simulated to produce the Figures. Values of the form a – b refer to the range of values covered with a non-constant step size. All other parameters with single values are held constant in simulations.

| Rate Name | Rate | Value |
|---------------------------------|-----------|----------------------|
| Secondary Transmission Rate | β | 1.0, 0.1, 0.04, 0.01 |
| Carrying Capacity | k | 120 |
| Growth Rate | r | 0.5 |
| Death Rate | μ | 0.1;0.5;0.1 |
| Immigration | ν | 0.1 |
| Infected Immigration Proportion | γ | 0.1 |
| Primary Transmission Rate | β_0 | 0 |
| Susceptible Active Capture | α | 0.1 |
| Infected Active Capture | α | 0.1 |
| Sample Target | m | 10.0 |

Table S3: Parameter values are shown for Figure 1 in the main text which demonstrates the effect of the death rate and transmission rate on the bias and variance of the prevalence estimate as well as the effect of the death rate on the population size and variance. 10^6 surveillance bouts are run of each combination and terminate when the sample target is reached, i.e. there is no time limit imposed. These parameters were implemented using the SDE version of the model.

| Rate Name | Rate | Value |
|---------------------------------|-----------|-----------|
| Secondary Transmission Rate | β | 1.0, 0.1 |
| Carrying Capacity | k | 120 |
| Growth Rate | r | 0.5 |
| Death Rate | μ | 0.4, 0.43 |
| Immigration | ν | 0.1 |
| Infected Immigration Proportion | γ | 0.1 |
| Primary Transmission Rate | β_0 | 0 |
| Susceptible Active Capture | α | 0 - 10 |
| Infected Active Capture | α | 0 - 10 |
| Sample Target | m | 10.0 |

Table S4: Parameter values are shown for Figure 2 in the main text which demonstrates the effect of the capture rate on the bias and variance of the prevalence estimate. 10^6 surveillance bouts are run of each combination and terminate when the sample target is reached, i.e. there is no time limit imposed. These parameters were implemented using the SDE version of the model.

| Rate Name | Rate | Value |
|---------------------------------|-----------|-----------|
| Secondary Transmission Rate | β | 1.0, 0.1 |
| Carrying Capacity | k | 120 |
| Growth Rate | r | 0.5 |
| Death Rate | μ | 0.4, 0.43 |
| Immigration | ν | 0.1 |
| Infected Immigration Proportion | γ | 0.1 |
| Primary Transmission Rate | β_0 | 0 |
| Susceptible Active Capture | α | 0.1 |
| Infected Active Capture | α | 0.1 |
| Sample Target | m | 1 - 10000 |

Table S5: Parameter values are shown for Figure 2 in the main text which demonstrates the effect of the sample size on the bias and variance of the prevalence estimate. 10^6 surveillance bouts are run of each combination and terminate when the sample target is reached, i.e. there is no time limit imposed. These parameters were implemented using the SDE version of the model.

| Rate Name | Rate | Value |
|---------------------------------|-----------|----------------------|
| Secondary Transmission Rate | β | 1.0, 0.1, 0.04, 0.01 |
| Carrying Capacity | k | 120 |
| Growth Rate | r | 0.5 |
| Death Rate | μ | 0.1;0.5;0.01 |
| Immigration | ν | 0.1 |
| Infected Immigration Proportion | γ | 0.1 |
| Primary Transmission Rate | β_0 | 0 |
| Susceptible Active Capture | α | 10, 1.0, 0.1, 0.01 |
| Infected Active Capture | A | 10, 1.0, 0.1, 0.01 |
| Sample Target | M | 10 |

Table S6: Parameter values are shown for Figure 3 in the main text which demonstrates the effect of the death rate and transmission rate, as well as the sample size and capture rate, on the probability of detecting disease. 10^6 surveillance bouts are run of each combination and terminate when the sample target is reached, i.e. there is no time limit imposed. These parameters were implemented using the SDE version of the model.

| Rate Name | Rate | Value |
|---------------------------------|-----------|-------------------------------------|
| Secondary Transmission Rate | B | 0.01,0.05,0.09,0.2,0.6, 1.0,2.0,5.0 |
| Carrying Capacity | K | 1;36.0;3.5 |
| Growth Rate | R | 0.5;23;2.5 |
| Death Rate | μ | 0.25;14.0;1.25 |
| Immigration | N | 1.0 |
| Infected Immigration Proportion | Γ | 0.01 |
| Primary Transmission Rate | β_0 | 0.01 |
| Susceptible Active Capture | A | 0.5 |
| Infected Active Capture | A | 0.5 |
| Sample Target | M | 10.0, 20.0 |

Table S7: Parameter values are shown for Figure 4 in the main text which demonstrates the effect of the transmission, death rate, birth rate, carrying capacity, as well as the sample size, on the probability of detecting disease. 1000 simulations were run per parameter combination with a time limit of 45. If the simulation did not reach the sample target within the time limit, the run is discarded and not used in the statistical calculations. If out of 1000 realisations a parameter combination ceases to reach the sample target at least 15 times, that parameter combination is discarded totally as the results are deemed to be unreliable. Increasing the time limit bears little to no effect on the amount simulations which reach the target sample, so the precise value of the time limit does not affect the results obtained from the model. These parameters were implemented using the Gillespie version of the model.

Appendix S3. Additional scenarios.

This appendix shows results for a set of scenarios complimentary to those in the main text. It is shown that the effects described in the main text are robust to three factors: population size; mode of secondary transmission and sample size.

Population size

The simulations in the main text are based on relatively small populations where fluctuations are driven only by demographic stochasticity. Here we simulate disease dynamics and surveillance in a population driven by environmental stochasticity (see below for details). This enables consideration of fluctuations in a much larger population since demographic fluctuations reduce with population size whereas environmental fluctuations do not. We show that in a population larger by a factor of approximately 10-100 compared with that described in the main text (Fig. 1 and Fig 3.), and using a sample size that is 10 times larger, the effects described are if anything greater. When compared with calculations based on assuming constant prevalence we see that the probability of detecting disease is reduced and estimates of prevalence are both biased and less precise (see Fig. S1 and Fig. S2).

The model used is as described in the main text but here the death rate is subjected to a correlated random walk based on a mean reverting Ornstein-Uhlenbeck process. With finite time step dt this is represented as

$$\mu(t + dt) = \mu(t) + (\mu_0 - \mu(t)) b_\mu dt + \sigma_\mu dB_\mu(t)$$

where $dB_\mu(dt), dB_\mu(2dt), \dots$ are independent identically distributed Gaussian random variables with zero mean and variance dt . The above equation is integrated along with the equations described in Appendix S1. After a burn-in period the equilibrium dynamics of this equation fluctuate around the mean μ_0 . The parameter b_μ controls the correlation in time of $\mu(t)$ and in the long run the variance in $\mu(t)$ is given by $\sigma_\mu^2 / 2 b_\mu$. The resulting fluctuations in mortality rate represent a range of environmental conditions from harsh to mild which drive fluctuations in the population size. The results shown in Fig. S1 and Fig. S2 are based on this model and the parameter values shown in Table S8. They show qualitatively the same effects seen in Fig. 1 and Fig. 3 in the main text.

| Rate Name | Rate | Value |
|---------------------------------|--------------|----------------------|
| Secondary Transmission Rate | B | 1.0, 0.1, 0.04, 0.01 |
| Carrying Capacity | K | 6000 |
| Growth Rate | R | 1.0 |
| Death Rate | μ_0 | 0.025;1.0;0.025 |
| Immigration | N | 0.1 |
| Infected Immigration Proportion | Γ | 0.1 |
| Primary Transmission Rate | β_0 | 0 |
| Susceptible Active Capture | A | 0.001 |
| Infected Active Capture | A | 0.001 |
| Sample Target | M | 100.0 |
| | b_μ | 0.4 |
| | σ_μ | 0.5 |

Table S8: Parameter values are shown for Figures S1 and S2. 10^6 surveillance bouts are run of each combination and terminate when the sample target is reached, i.e. there is no time limit imposed. These parameters were implemented using the SDE version of the model incorporating the stochastic variation in the death rate described above.

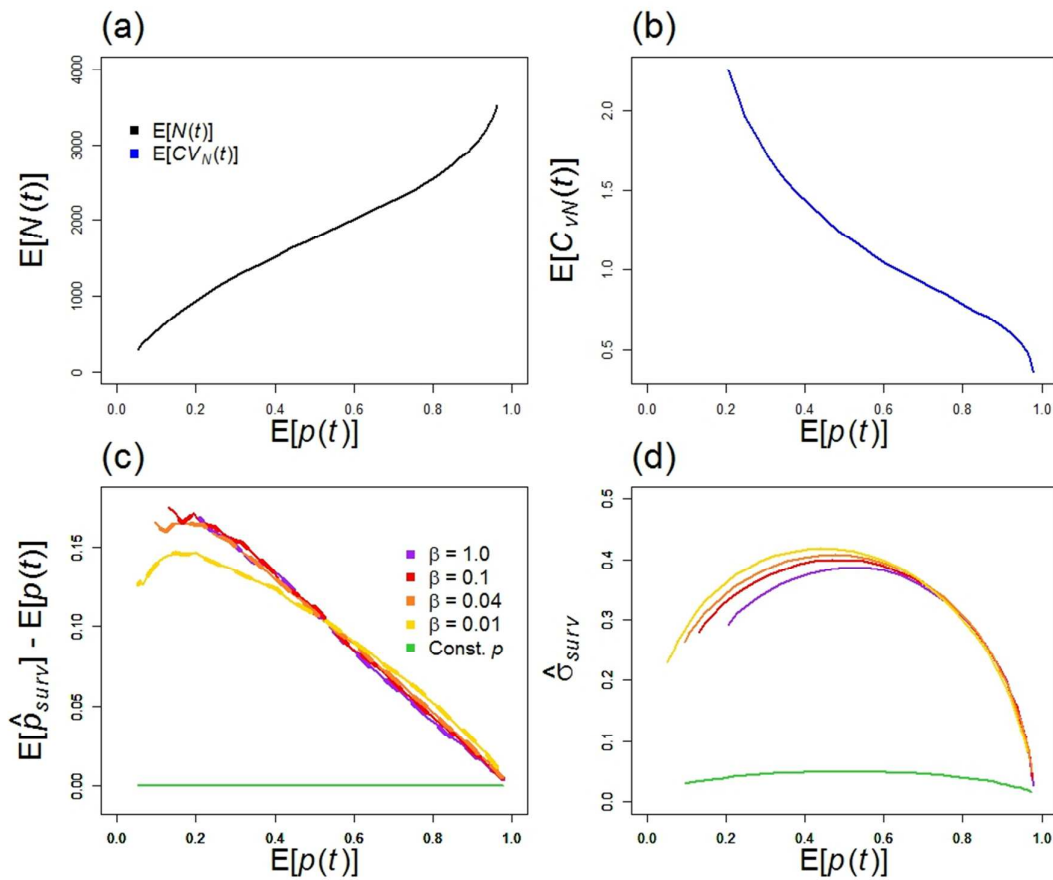


Figure S1: This figure is the counterpart to Fig. 1 in the main text but for the large population simulations with fluctuating death rate described above. The typical population sizes range from around 500-3000 and the sample size used is 100.

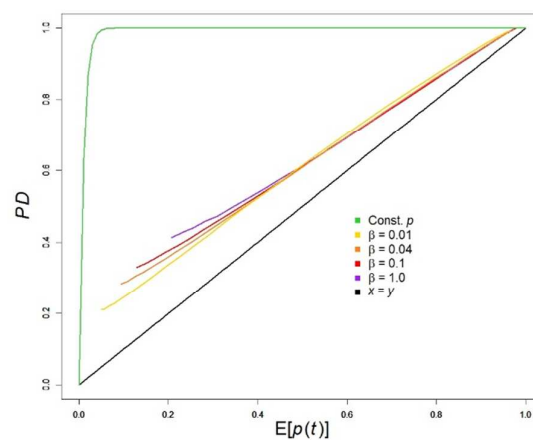


Figure S2 Probability of disease detection. This plot is the counterpart to Fig 3c in the main text but for the large population described above.

Frequency dependent transmission

The scenario simulated here is identical to that shown in Figs 1 and 3 in the main text except that here disease transmission is frequency dependent such that secondary infections occur at rate

$$\tilde{\beta} \frac{S(t) I(t)}{N(t)}$$

Recall that the total population size at time t is $N(t)$ and is made up of $S(t)$ susceptible and $I(t)$ infectives. Contrasting the above formulation with the density dependent transmission rate $\beta S(t) I(t)$ it is clear that to ensure comparable rates of transmission we require $\tilde{\beta} \approx \beta N$. Therefore to ensure comparability between the simulations of frequency and density dependent transmission the contact rate $\tilde{\beta}$ is given by

$$\tilde{\beta} = \beta K \frac{(r - \mu)}{r}$$

where β is the density dependent transmission rate and $K (r - \mu)/r$ is the equilibrium population size derived from the deterministic version of the model.

The results shown in Fig. S3 and Fig S4 show that the effects described in the main text are just as evident in the case of frequency dependent transmission as they are for density dependent transmission.

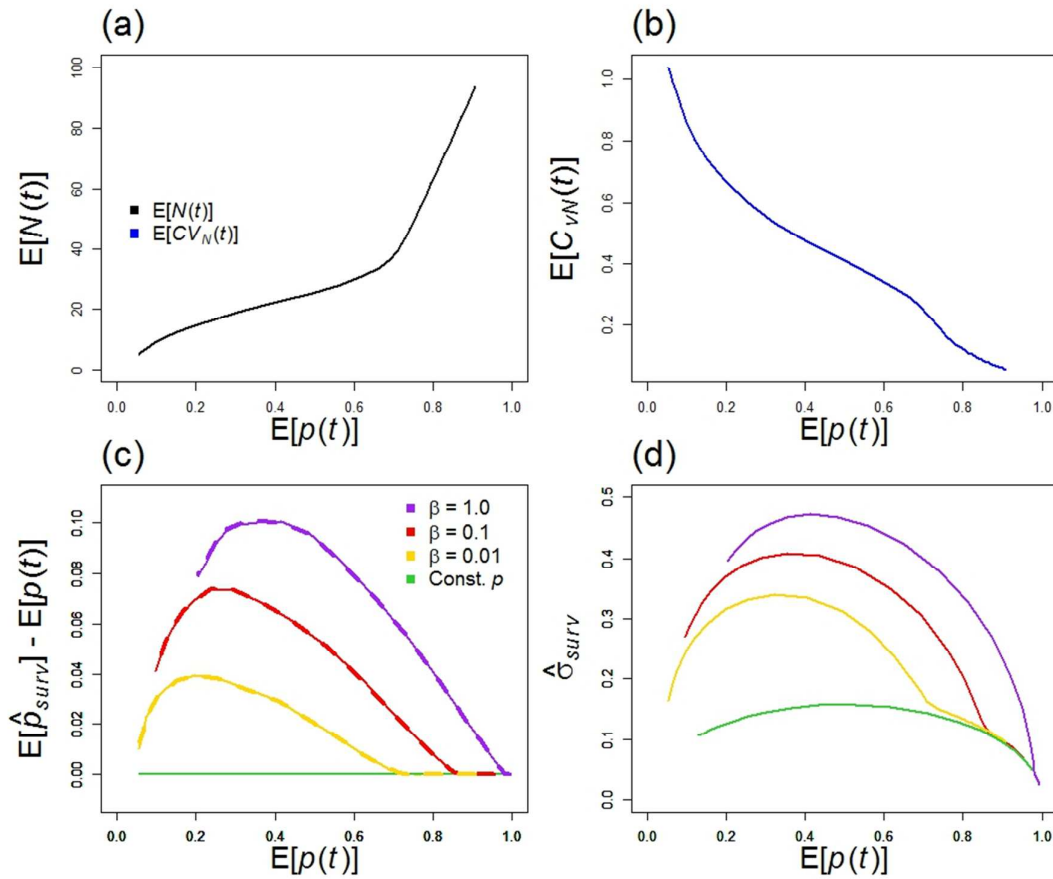


Figure S3: Equivalent to Fig 1 in the main text but for the frequency dependent transmission described above described above.

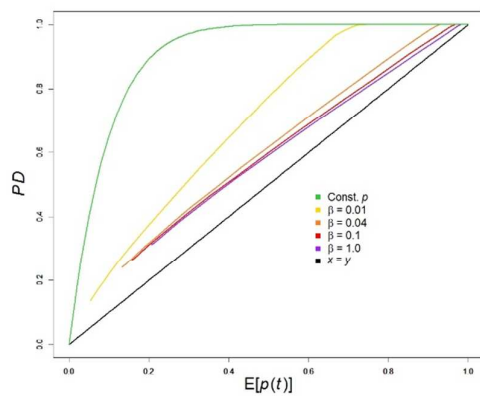


Figure S4 Probability of disease detection. This plot is the counterpart to Fig 3c in the main text but for the frequency dependent transmission described above described above.

Sample size:

Here we show results from a scenario identical to that shown in Figures 1 and 3 of the main text except that the sample size is increased from 10 to 20 and 50. In this scenario the population is typically between 10 and 40 individuals so although these sample sizes may seem low they represent a large fraction of the population. The figures below demonstrate that sample size has little effect on the degradation in the performance of surveillance. Thus these results support the conclusion drawn from Fig. 2 in the main text.

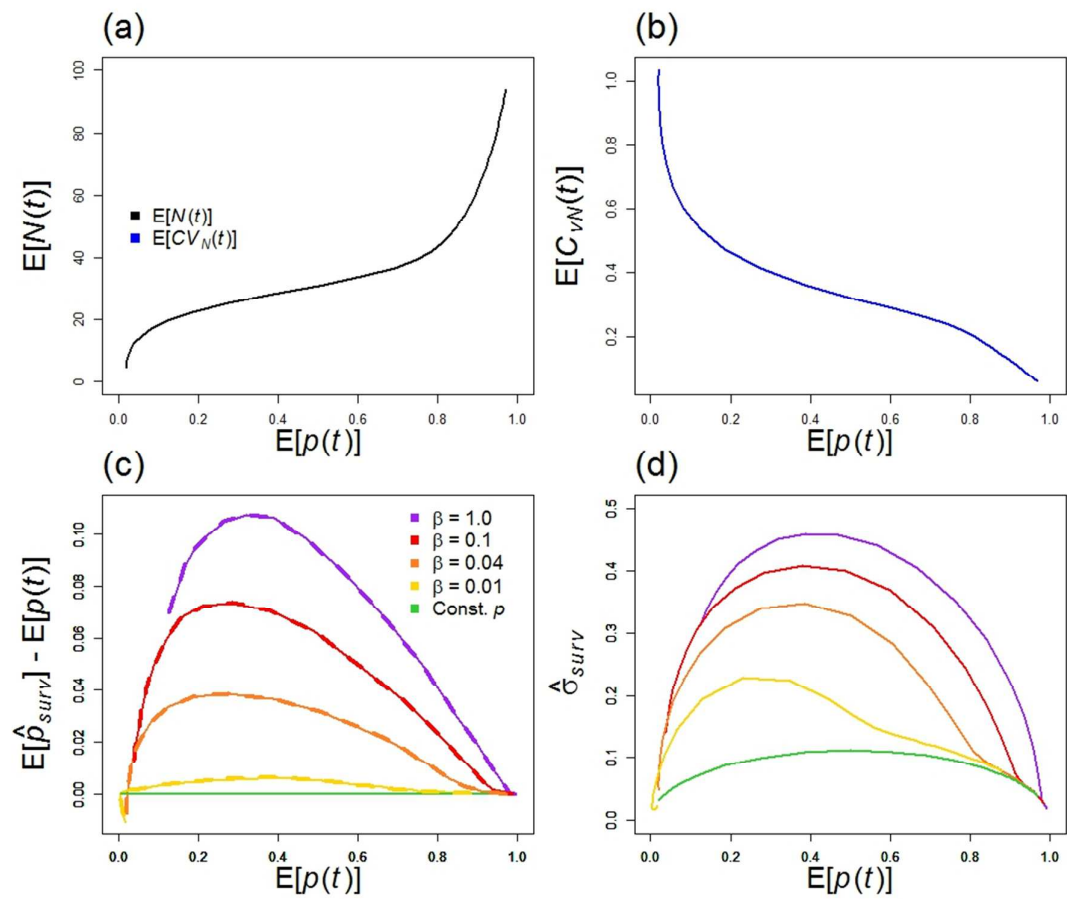


Figure S1: This figure depicts the scenario shown in Figure 1 of the main text but with sample size 20.

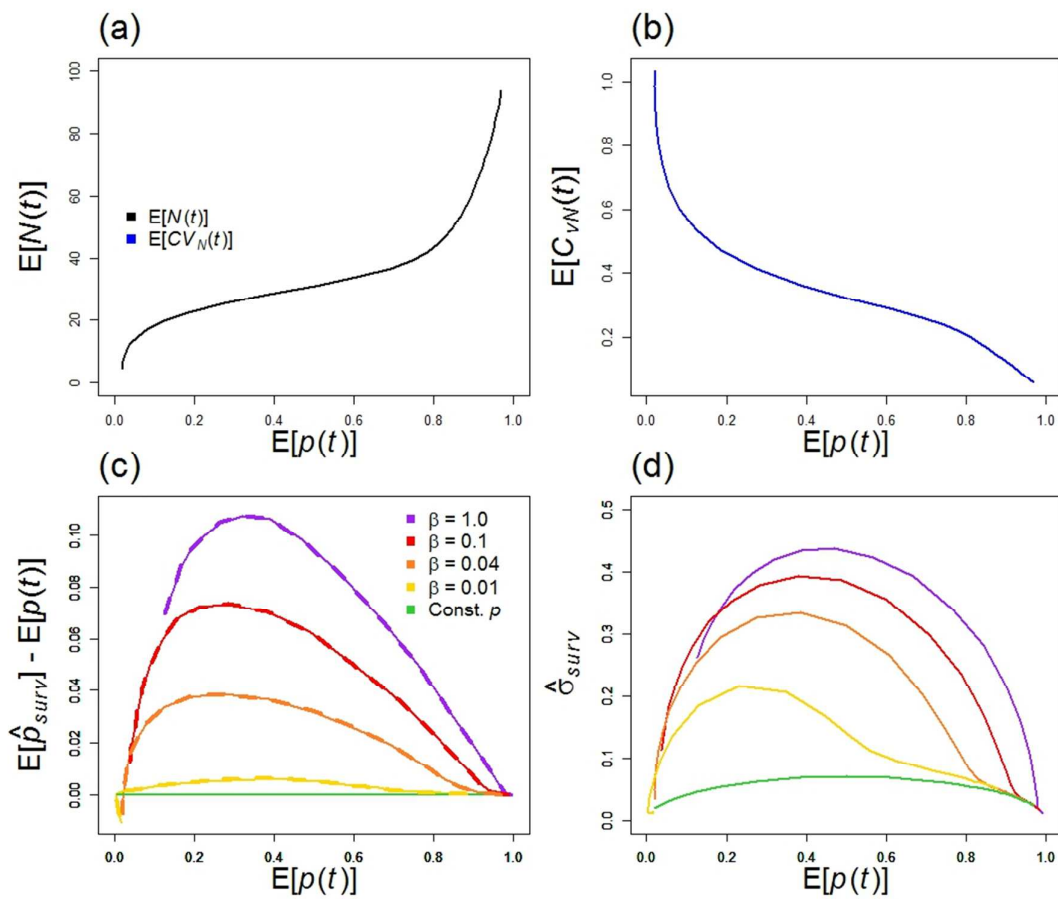


Figure S2: This figure depicts the scenarios shown in Figure 1 of the main text but with sample size 50.

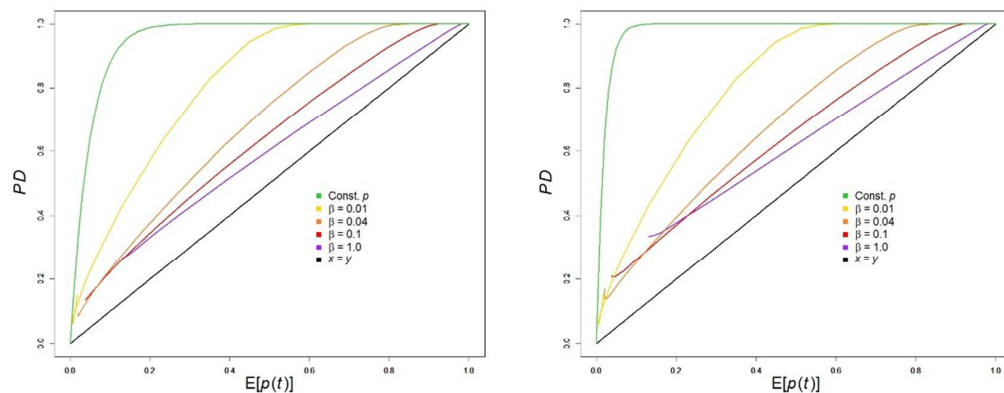


Figure S3: Probability of detection. This plot is the counterpart to Fig 3c in the main text but for increased sample sizes. The plot on the right shows sample size 20 and that the right 50 whereas Fig 3c is based on sample size 10.

Appendix S4. Analysis of disease detection probability

In many cases the primary goal of wildlife disease surveillance is detection of disease rather than quantification of prevalence. This is true, for example, for emerging or re-emerging disease, where detection is a precursor to further action, which would include heightened surveillance. If prevalence is assumed constant and equal to the long term average prevalence $E[p]$ of the wildlife disease system, then the probability that disease is detected in a sample of size m is given by:

$$PD^{Bin} = f(E[p], m) = 1 - (1 - E[p])^m$$

This formula, based on simple binomial arguments, and variants that also assume constant prevalence, are the standard basis for sample size calculations (see e.g. Fosgate 2009). However, if prevalence fluctuates PD^{Bin} is a misleading estimate of the probability of detection.

In real systems, prevalence varies with time; therefore, when conducting surveillance, the prevalence values will vary at the times when each of the m samples are collected. Nonetheless, for simplicity here we assume that the prevalence during a given surveillance bout (i.e. the collection of m consecutive samples) is constant, and denoted p . Fig. 3a (see main text) compares the probability of detection measured from simulations with two approximations. The first approximation accounts for fluctuations both within and between surveillance bouts and the second only that between surveillance bouts. These results indicate that accounting only for fluctuations between surveillance bouts is an accurate approximation. Therefore, the expected probability of detection for sample size m is defined as

$$PD = E[f(p, m)] = E[1 - (1 - p)^m]$$

where the expectation is over the between bout prevalence distribution $P(p)$ which accounts only for prevalence fluctuations between surveillance bouts. For a single sample $m = 1$, the above equation for PD reduces to a linear form, so that $PD = PD^{Bin} = E[p]$. However, if $m > 1$, then the equation for PD is non-linear, and therefore $PD \neq PD^{Bin}$.

To illustrate this, we Taylor expanded PD by assuming that the difference between the bout prevalence (p) and the long term average prevalence is small i.e. $p = E[p] + \Delta p$. Then, noting that $E[\Delta p] = 0$ and $var[p] = E[\Delta p^2]$ and ignoring terms containing higher powers of Δp , this yields

$$PD \cong PD^{Bin} + \frac{1}{2}var[p] \frac{\partial^2 f(p, m)}{\partial p^2} \Big|_{p=E[p]}$$

This suggests (to leading order in the expansion) that the true probability of detection will be lower than PD^{Bin} , since the second derivative $\partial^2 f(p, m) / \partial p^2 = -m(m-1)(1-p)^{m-2}$ is negative for sample size $m > 1$ and $p = E[p]$. In addition, the size of this deviation depends on the sample size and the variance in prevalence. Although these conclusions are broadly correct, when compared with simulation results, the above Taylor expansion does not provide an accurate approximation of the probability of detection. However, analytic progress can be made, with the following alternative approach. The approximation $(1-p)^m \approx e^{-pm}$ holds for m large (and is already accurate even for $m = 10$) and enables us to write the probability of detection as:

$$PD = 1 - E_p[(1-p)^m] \cong 1 - E[e^{-pm}] = 1 - M_p(m)$$

where $M_p(m) \equiv E[e^{-pm}]$ is the moment generating function associated with the between bout prevalence distribution $P(p)$. This suggests that if we could parameterise a suitable distribution to approximate $P(p)$ then we could use the corresponding moment generating function to calculate the probability of detection.

Fig. 3a (main text) suggests that a moment-generating function approximation (see last equation above) based on the actual distribution of prevalence between surveillance bouts would be an accurate approximation. Fig. 3b illustrates this approximation using an assumed gamma distribution, parameterised with the mean and variance of $P(p)$. Although the gamma approximation is not completely successful, it does provide a more accurate prediction of PD than PD^{Bin} . This could be used to improve sample size calculations in situations where simulation is not possible, but information about prevalence fluctuations is available. Moreover, the results of Fig. 3a show that such approximations could be improved by assuming a more accurate representation of the prevalence distribution $P(p)$.